Chemical Engineering Journal 144 (2008) 124–137

Contents lists available at ScienceDirect

Chemical Engineering Journal

journal homepage: www.elsevier.com/locate/cej

Experimental investigation of sheet flexibility of layered double hydroxides: One-pot morphosynthesis of inorganic intercalates

Bo Li, Jing He*, David G. Evans

State Key Laboratory of Chemical Resource Engineering, Beijing University of Chemical Technology, Beijing 100029, PR China

ARTICLE INFO

Article history:
Received 12 March 2008
Received in revised form 11 June 2008
Accepted 29 June 2008

Keywords:
Layered double hydroxides
Morphosynthesis
Sheet flexibility
In situ transformation of interlayer anions

ABSTRACT

The sheet flexibility of layered double hydroxides (LDHs) has been investigated experimentally using co-precipitation and urea hydrolysis methods in an aqueous solution of long-chain anion surfactant in this work. Using dodecylsulfate (DS) anion as morphology-controlling agent, layer-bended or contorted Mg/Al-LDH is obtained successfully. The morphology of bent layers is retained during either *in situ* decomposition of interlayer DS to SO_4^{2-} or ion exchange of interlayer DS by CO_3^{2-}. The direct synthesis of the layer-distorted LDHs intercalated with small inorganic anions is quite difficult. It has been achieved using layer-bended LDHs pillared with bulky organic anions as precursors in this paper. The morphosynthesis is expanded to Co/Al and Ni/Al-LDHs, indicative of the general flexibility of this kind of anionic clays.

1. Introduction

Flexible materials generally include polymers, colloids, amphiphilic aggregates, and liquid crystals. Experimental investigation has testified that the host layers of some layered materials such as montmorillonite [1], graphite [2], and mono-metal anionic layered materials [3] are also flexible and could be curved. The flexibility of a material is directly related to the vibration and rotation of chemical bonds. He and Kunitale [4] concluded that when the sheets are thin enough, the layered inorganic materials could be deformed by applying a bending force which weakens and deforms the bonding interaction on the atomic and molecular scale. The flexibility of clay layers can be reflected by the process of either staging or layer bending. Among the few reported cases, the staging explained by Daumas and Hérold model [5] often occurs in intercalated graphite compounds, showing draped and flexible layers [6,7].

Different from mono-metal layered materials, layered double hydroxides (LDHs) are a class of anionic clays whose structure is based on brucite ($Mg(OH)_2$)-like layers in which some of the divalent cations have been replaced by trivalent ions giving positively charged sheets. This charge is balanced by intercalated anions in the hydrated interlayer regions. LDHs can be represented by the general formula $[M^{II}_{1-x}M^{III}_x(OH)_2]^{x+}(A^{n-})_{x/n}yH_2O$, where M^{II} are divalent cations such as Mg, Ni, Co, Cu, and Zn, M^{III} are trivalent cations such as Al, Fe, Cr, and Ga, and A^{n-} are interlayer anions that consist of a wide variety of inorganic and organic species [8–10]. Various preparation methods, such as co-precipitation [10–13], urea hydrolysis [14–17], separate nucleation and aging [18], and ion-exchange [19], have been developed and attempted to control the crystal growth of LDHs, as reviewed recently [20]. But non-bended planar layers [21–23] have always been observed, which seems indicative of the hardness and rigidity of the layers [24,25]. The Rüdorff model of the staging was always used to explain the rigidity of LDH layers [26]. Theoretically, however, molecular dynamic investigation has pointed out that LDHs are not as flexible as graphite but more flexible than smectite clays like montmorillonite [27]. So LDHs is supposed to be flexible in nature and the morphosynthesis of layer-bended LDH is possible to be achieved experimentally through appropriate techniques.

The anion-exchangeable property of LDHs allows this kind of two-dimensional material to be intercalated by a vast array of guests [28–31], facilitating LDHs with potential application as adsorbents, ion-exchange agents, additives in polymer-based composites, [32] as well as supports for catalytic sites [33,34] and biomolecules such as urease [29], lipase [35] and DNA [36]. Long-chain anionic surfactants can serve as either guests for LDH intercalation [37,38] or candidates for self-assembly to micelles (or even liquid crystal phase) in aqueous solution [39,40]. The features are utilized in this work to enlarge the interlayer distance and further induce the sheet-growth of LDHs. Multiple effects of surfactant anions have been found in LDHs' crystal growth in our recent work [41]. In this paper, long-chain anionic surfactants with similar structures and properties, including sodium dodecylsulfate (SDS, $C_{12}H_{25}SO_4Na$), sodium dodecylsulfonate (SAS, $C_{12}H_{25}SO_3Na$) and

* Corresponding author. Tel.: +86 10 64425280; fax: +86 10 64425385.
E-mail addresses: jinghe@263.net.cn, hejing@mail.buct.edu.cn (J. He).

1385-8947/$ – see front matter © 2008 Elsevier B.V. All rights reserved.
doi:10.1016/j.cej.2008.06.031

Table 1
Indexing of XRD patterns for Mg/Al-LDHs synthesized in different SDS concentrations by the urea hydrolysis method aging for 2 h

SDS concentration (mol/L)	d_{003} (nm)	d_{006} (nm)	d_{009} (nm)	d_{110} (nm)	Content of DS (%)
0.01	2.80	1.38	0.912	0.1519	36.40
0.015	2.77	1.34	0.889	0.1519	36.84
0.0175	2.78	1.32	0.909	0.1521	40.32
0.02	2.78	1.32	0.905	0.1523	42.00

bis(2-ethylhexyl) sulfosuccinate (AOT, $C_{20}H_{37}SO_7Na$), are applied to control the crystal growth of LDHs. The layer flexibility of this kind of clays has been clearly revealed experimentally. Besides the flexibility of host-layers, the particle morphology and intercalation structure are also investigated in detail.

The experimental investigation of layer flexibility and morphosynthesis of LDH materials are believed to be of great importance and significance for their potential applications related to soft matters such as polymers [32], proteins [29,35], and other bio-macromolecules [36,42].

2. Experimental

2.1. Materials and preparation procedures

Magnesium nitrate hexahydrates ($Mg(NO_3)_2{\cdot}6H_2O$), aluminium nitrate nonahydrates ($Al(NO_3)_3{\cdot}9H_2O$), nickel nitrate hexahydrates ($Ni(NO_3)_2{\cdot}6H_2O$), cobalt nitrate hexahydrates ($Co(NO_3)_2{\cdot}6H_2O$), sodium carbonate (Na_2CO_3), sodium sulfate (Na_2SO_4), sodium hydroxide (NaOH), sodium dodecylsulfate ($C_{12}H_{25}SO_4Na$, SDS), sodium dodecylsulfonate ($C_{12}H_{25}SO_3Na$, SAS), bis(2-ethylhexyl) sulfosuccinate ($C_{20}H_{37}SO_7Na$, AOT), and urea, purchased from Beijing Chemical Regents Co. are all of analytical purity and used without further purification. Deionized water, used in the precipitation and aging of LDHs, had been boiled to remove dissolved CO_2 before use to avoid the competitive intercalation of carbonate anion.

The urea hydrolysis synthesis of Mg/Al-LDHs in sodium dodecylsulfate (SDS) solution: 0.0016 mol $Mg(NO_3)_2$, 0.0008 mol $Al(NO_3)_3$ and 0.0016 mol SDS were firstly mixed in 80 mL deionized water in a 100 mL Teflon autoclave. 0.0079 mol urea was immediately added into the above solution and stirred quickly using a magnetic stirrer. After 20 min, the mixed solution was heated at 150 °C for 1, 2, 3, 6, 12, 24, and 120 h, respectively. White powdery products were collected after being extensively washed with deionized water and ethanol to remove superfluous surfactant and other inorganic ions. Especially, the solid in 120 h aging was washed in alcohol medium for 7 days to thoroughly remove the adsorbed surfactant. Changing the concentration of SDS to 0.010, 0.015 and 0.0175 M, respectively, Mg/Al-LDHs were synthesized using the same method. Changing [Mg^{2+}] to 0.002 M and [Al^{3+}] to 0.001 M, Mg/Al-LDHs were synthesized in 0.02 M SDS solution. The aging was performed at 150 °C for 24, 48, 72 and 120 h, respectively.

The synthesis of Mg/Al-LDHs in SAS or AOT aqueous solution and Ni/Al-LDHs or Co/Al-LDHs in SDS or SAS aqueous solution were carried out following the same procedure as described above. The aging time was 24 h at 150 °C.

The co-precipitation synthesis of Mg/Al-LDHs in SDS aqueous solution: 0.0016 mol $Mg(NO_3)_2$, 0.0008 mol $Al(NO_3)_3$ and 0.0016 mol SDS were firstly mixed in 40 mL deionized water in a 100 mL Teflon autoclave. Forty microliters aqueous solution of sodium hydroxide (0.096 M NaOH) was immediately added into the above solution under thorough agitation. The solution was finally adjusted to pH 9.0 using 3.0 M NaOH solution. After 20 min, the white slurry was heated at 150 °C for 24, 72, and 240 h, respectively. The solid in 240 h aging was washed in alcohol medium for 7 days to thoroughly remove the adsorbed surfactant.

The synthesis of Mg/Al-CO_3^{2-} LDH in SDS aqueous solution: 0.0016 mol $Mg(NO_3)_2$ and 0.0008 mol $Al(NO_3)_3$ were firstly mixed in 20 mL deionized water in a 100 mL Teflon autoclave. Twenty microliters aqueous solution of 0.0016 mol Na_2CO_3 and 0.00384 mol NaOH was immediately added into the above solution under thorough agitation. The solution was finally adjusted to pH 9.0. After 20 min, 40 mL 0.04 M SDS solution was added into the above white slurry solution. The resulting slurry was heated at 150 °C for 24 h. The ion-exchange of Mg/Al-SO_4^{2-} LDH precursor with DS anion was performed following the same procedure except that Na_2SO_4 substituted for Na_2CO_3.

The synthesis of Mg/Al–SO_4^{2-} LDH in the absence of surfactant: 0.0016 mol $Mg(NO_3)_2$ and 0.0008 mol $Al(NO_3)_3$ were firstly mixed in 40 mL deionized water in a 100 mL Teflon autoclave. Forty microliters aqueous solution of 0.0016 mol Na_2SO_4 and 0.00384 mol NaOH was immediately added into the above solution under thorough agitation. The solution was finally adjusted to pH 9.0. After 20 min, the white slurry was heated at 150 °C for 24 h.

The concentrations of Mg^{2+} (Ni^{2+}, Co^{2+}), Al^{3+}, and SDS (SAS, AOT) are 0.02, 0.01, and 0.02 M, respectively, in the synthesis solution if not specially defined.

2.2. Instrument and characterization

Powder X-ray diffraction (XRD) data were collected on a Shimadzu XRD-6000 powder diffractometer, using Cu Kα ($\lambda = 0.1542$ nm) radiation (40 kV and 30 mA) between 2 and 70° with a scanning rate of 5° min^{-1} and step size of 0.02°. Glass holder was used for all samples in XRD characterization. The FT-IR spectra

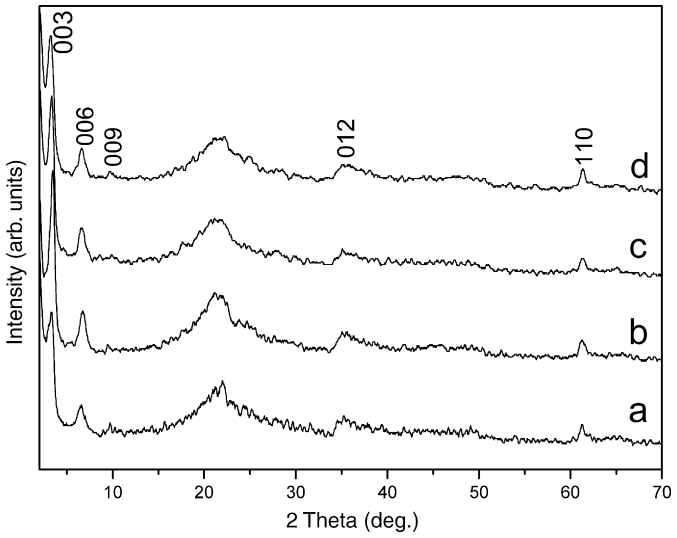

Fig. 1. XRD patterns of Mg/Al-LDHs aging for 2 h in (a) 0.01 M; (b) 0.015 M; (c) 0.0175 M; (d) 0.02 M SDS aqueous solutions by the urea hydrolysis method.

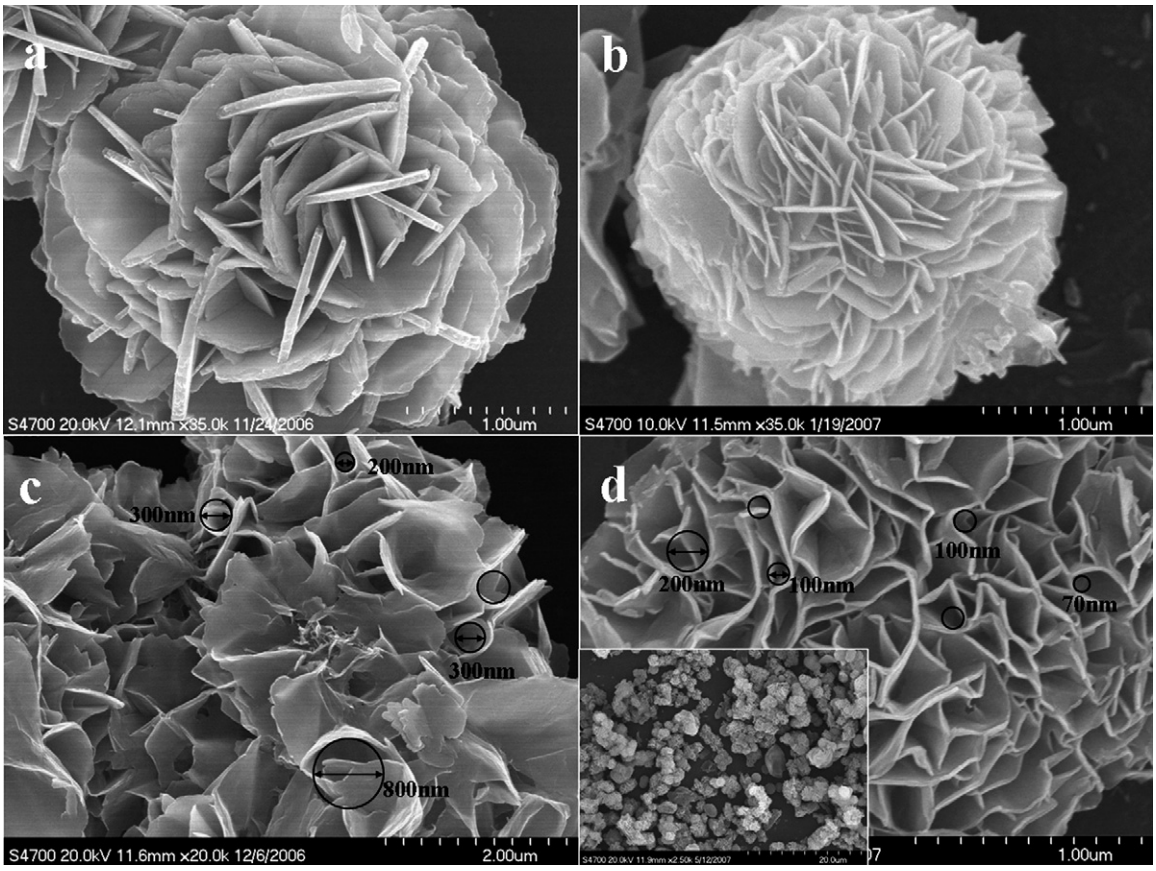

Fig. 2. SEM images of Mg/Al-LDHs aging for 2 h in (a) 0.01 M; (b) 0.015 M; (c) 0.0175 M; (d) 0.02 M SDS solution by the urea hydrolysis method.

were recorded on a Bruker Vector 22 spectrometer at a resolution of 4 cm^{-1}, the samples being pressed into disks with KBr. Elemental analyses of Mg and Al were performed by ICP emission spectroscopy by dissolving the samples in dilute H_2SO_4. C, H, and O micro-analysis was carried out using an elemental analyzer (Elementar Co., Vario El). SEM micrographs were taken on a HITACHI S-4700 scanning electron microscope. TEM micrographs were taken on a JEM-3010 transmission electron microscope. The sample for TEM characterization was prepared by dipping carbon coated copper TEM grids with dilute ethanol suspensions of the sample powder.

3. Results and discussion

3.1. Sheet deformation of LDHs intercalated with surfactant anions

The synthesis of LDHs intercalated with surfactant anions has been of great interest. But much attention was paid on the crystal structures, properties and applications [37,38,43]. In this work, three kinds of widely used anionic surfactants (SDS, SAS and AOT) are applied in LDHs' synthesis to investigate the flexibility of LDHs sheets. Mg/Al-LDHs were first synthesized under different SDS

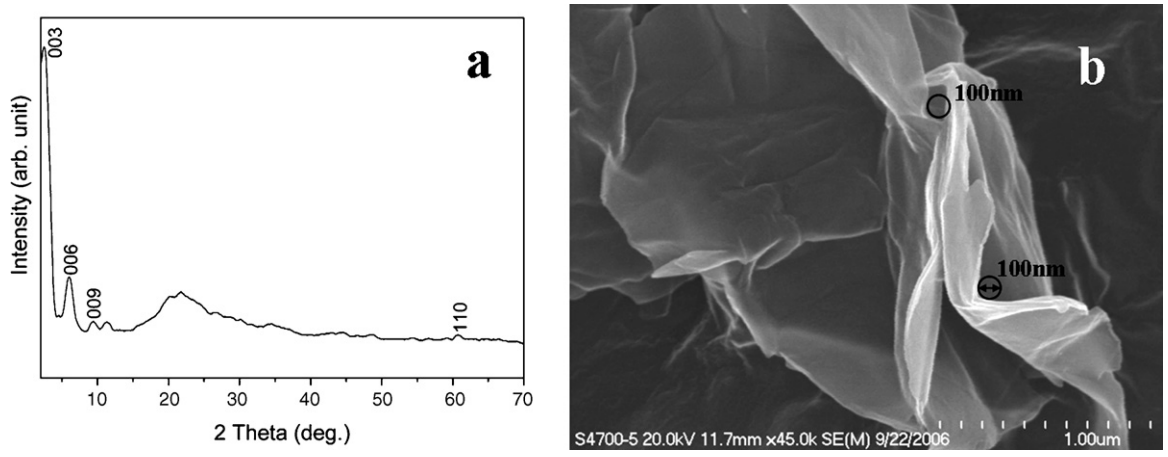

Fig. 3. XRD pattern (a) and SEM image (b) for Mg/Al-LDH synthesized in 0.002 M Mg^{2+}, 0.001 M Al^{3+} and 0.02 M SDS solution aging for 24 h by the urea hydrolysis method.

Table 2
Indexing of XRD patterns for LDHs synthesized by the urea hydrolysis method aging for 24 h

LDHs samples	d_{003} (nm)	d_{006} (nm)	d_{009} (nm)	d_{110} (nm)
Mg/Al-AS LDH	2.54	1.23	0.810	0.1520
Mg/Al-DS LDH	2.79/0.765[a]	1.38/0.379[a]	0.894	0.1523
Mg/Al-AOT LDH	2.56	1.21	0.799	0.1520
Co/Al-DS LDH	2.72/0.758[a]	1.36/0.379[a]	0.903	0.1535
Co/Al-AS LDH	2.65	1.25	0.796	0.1538
Ni/Al-DS LDH	2.72/0.781[a]	1.37	0.872	0.1518

[a] (0 0 *l*) of CO_3^{2-} anion-intercalated LDH.

Table 3
Indexing of XRD patterns for Mg/Al-LDHs synthesized in 0.02 M SDS solution by the urea hydrolysis method

Aging time (h)	d_{003} (nm)	d_{006} (nm)	d_{009} (nm)	d_{110} (nm)
1	3.21			
2	2.78[a]	1.32[a]	0.905[a]	0.1523
3	2.75[a]/0.769[b]	1.29[a]/0.381[b]	0.851[a]	0.1519
24	2.72[a]/0.769[b]	1.27[a]/0.382[b]	0.834[a]	0.1523
120	0.767[b]	0.381[b]	0.868[a]	0.1523

[a] (0 0 *l*) of DS anion-intercalated LDH.
[b] (0 0 *l*) of CO_3^{2-} anion-intercalated LDH.

concentrations by the urea hydrolysis method. Fig. 1 shows the XRD patterns of the resulting solids. The (0 0 3), (0 0 6), (0 0 9) and (1 1 0) reflections characteristic of dodecylsulfate ($C_{12}H_{25}SO_4^-$ and DS) intercalated LDHs, similar to reported previously [43–46], are clearly observed. The basal spacing (d_{003}) is all calculated as approximately 2.78 nm. All of the samples exhibit turbostatic disorders as can be seen from the saw-toothed peaks at $2\theta = 34^\circ$ and 61°corresponding to the (0 1 2) and (1 1 0) reflections, respectively. A broad peak centered at 22° is observed for all the samples. It remains unchanged using either glass or aluminum sample holder for XRD test. Leroux et al. [47] and Zammarano et al [48] considered it came from the absorbed surfactant on the LDHs surface. But Jaubertie et al. [49] found this broad peak only existed in wet delaminated LDH sample. It is found in our experiment that the intensity of the broad peak is not reduced at all by thoroughly wash in alcohol medium to remove the adsorbed surfactant (Fig. S1 in Supporting Information). We propose that the observed broad peak around 22° originate from the enlargement of interlayer spacing by DS intercalation. That is, for DS-intercalated LDHs, the distance between adjacent sheets in *c* direction is large enough to grant LDH sheets analogously delaminated features. The lattice parameters in Table 1 indicate that the basal spacing (d_{003}) has negligible change with SDS concentration, indicative of the same arrangement of DS in the interlayer galleries. The full length of dodecylsulfate (2.08 nm) [43–45] plus the thickness of host-layer (0.48 nm) [44] turns out to be 2.56 nm, smaller than the basal spacing observed (2.77–2.80 nm), indicative of a bilayer arrangement of the interlayer $C_{12}H_{25}SO_4^-$ with the alkyl chains partially interdigitating perpendicularly.

Table 4
Indexing of XRD patterns for Mg/Al-LDH synthesized in 0.02 M SDS solution by the urea hydrolysis method

Aging time (h)	d_{003} (nm)	d_{006} (nm)	d_{009} (nm)	d_{110} (nm)
24	3.15[a]	1.46[a]	0.95[a]	0.152
48	0.85[a]	0.43[a]		0.152
72	0.98[a]/0.79[b]	0.46[a]/0.42[b]		0.152
120	0.77[b]	0.38[b]		0.153

$[Mg^{2+}]/[Al^{3+}] = 0.002\ M/0.001\ M$.
[a] (0 0 *l*) of DS anion-intercalated LDH.
[b] (0 0 *l*) of CO_3^{2-} anion-intercalated LDH.

Fig. 2 shows the SEM images of the DS-intercalated Mg/Al-LDHs using the urea hydrolysis method. The morphology of LDHs particles is diversified depending on the SDS concentration in the synthesis mixture. When [SDS] ≤ 0.015 M (0.01 and 0.015 M herein), uniform conventional sand-rose-like aggregates of sheet-planar particles (Fig. 2a and b) are observed. In the case of [SDS] = 0.0175 M, the aggregates of LDHs particles with sheet-curved or bended morphology (Fig. 2c) are observed. Increasing [SDS] to 0.02 M enhances the curvature of LDHs sheets (Fig. 2d). The curvature radii of bent layers reduce from mostly 150 nm (Fig. 2c) to mostly 50–100 nm (Fig. 2d) when SDS concentration increases from 0.0175 to 0.02 M. In this synthesis system, 0.01 M SDS is demanded as interlayer anions for stoichiometric compensation for the positive charges of LDHs layers arising from Al^{3+}. It is believed therefore that to obtain layer-bended Mg/Al-LDHs, more dodecylsulfate has to be introduced into the synthesis solution than needed for intercalation. The particles get thinner along the stacking direction with increasing SDS concentration. But the contents of DS anion in the final products change only slightly from 36.40% to 42.00% (Table 1). The slab thickening with decreasing SDS content could be explained as the less restriction effects on LDH particle growth by the surfactant anions in excess of intercalation. Decreasing $[Mg^{2+}]$ and $[Al^{3+}]$ to 0.002 M and 0.001 M, well crystallized DS-intercalated Mg/Al-LDHs (Fig. 3a) showing bent layers (Fig. 3b) are also synthesized successfully.

The above observations indicate that the layer of Mg/Al-LDH is flexible enough to be deformed or bended, which experimentally supports the theoretical speculation [27]. LDHs are a kind of host–guest composites, in which the host layers contain various metal cations and the interlayer guests are exchangeable inorganic or organic anions. To investigate whether the layer flexibility is of generalization for LDHs materials, and also demonstrate the similar inducing function of anion surfactants, three surfactants are applied in the morphosynthesis of Mg/Al, Co/Al, and Ni/Al-LDHs materials.

Fig. 4 shows the XRD patterns of Mg/Al, Co/Al and Ni/Al-LDHs synthesized in three kinds of surfactant solutions. The obvious (0 0 *l*) reflections show that dodecylsulfonate (DS), dodecylsulfate (AS) and bis(2-ethylhexyl) sulfosuccinate (AOT) anions have been intercalated into the interlayer galleries of Mg/Al, Co/Al

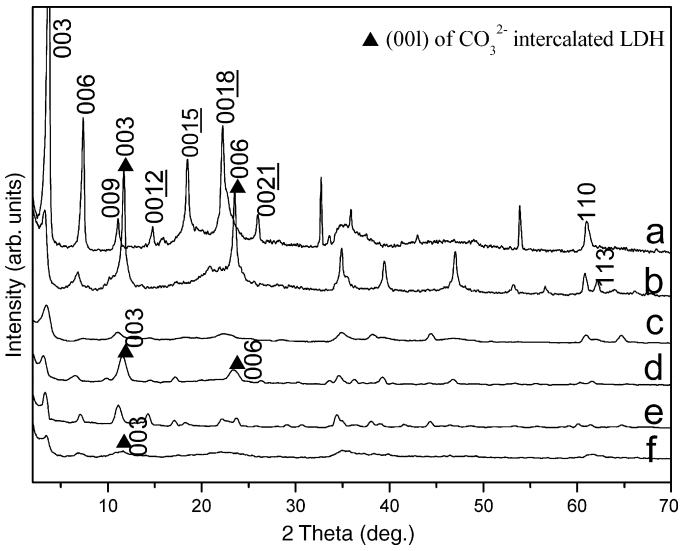

Fig. 4. XRD patterns of (a) AS-intercalated Mg/Al-LDH; (b) DS-intercalated Mg/Al-LDH; (c) AOT-intercalated Mg/Al-LDH; (d) DS-intercalated Co/Al-LDH; (e) AS-intercalated Co/Al-LDH; (f) DS-intercalated Ni/Al-LDH synthesized by urea hydrolysis method aging for 24 h at 150 °C.

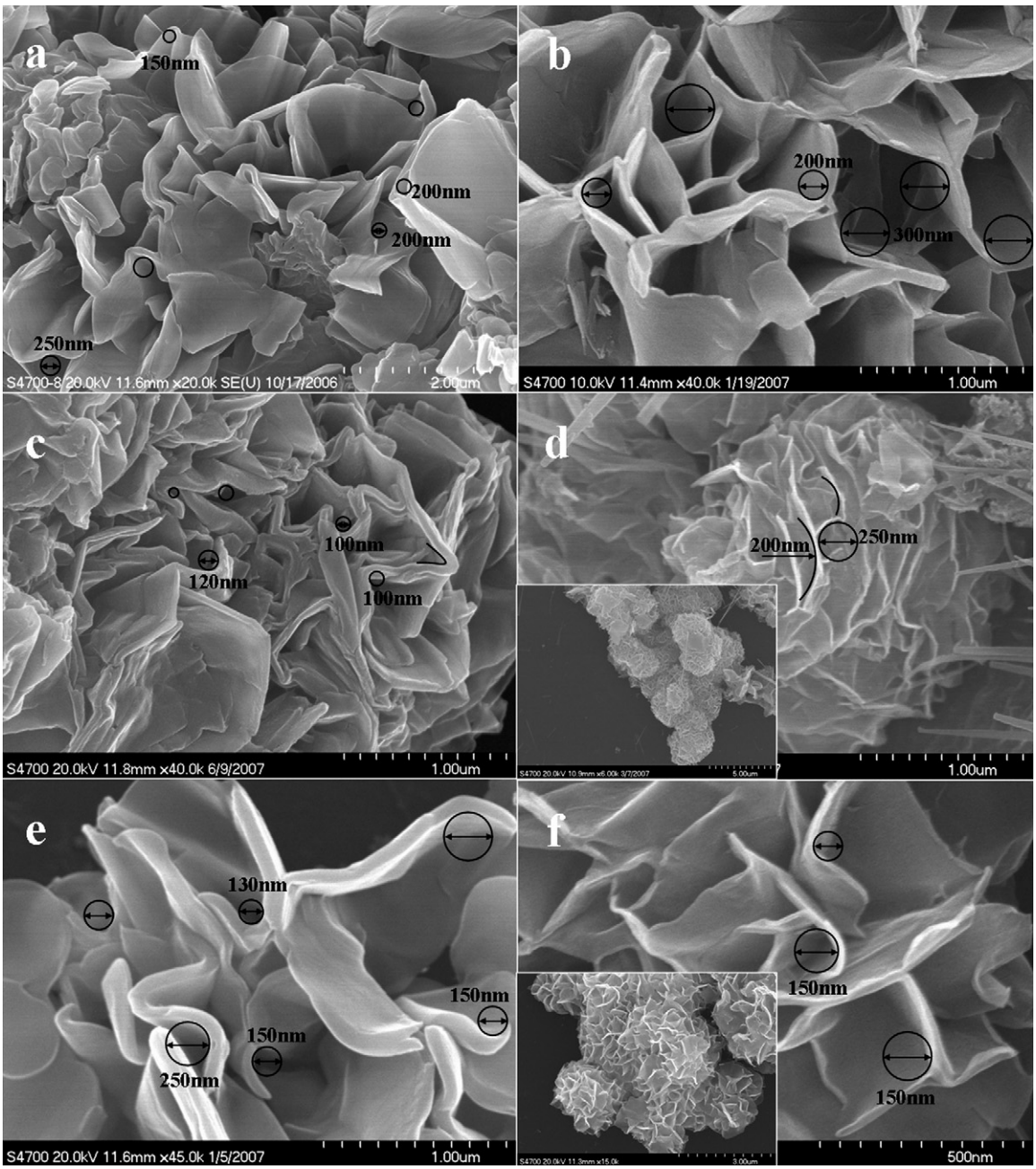

Fig. 5. SEM images of (a) AS-intercalated Mg/Al-LDH; (b) DS-intercalated Mg/Al-LDH; (c) AOT-intercalated Mg/Al-LDH; (d) DS-intercalated Co/Al-LDH; (e) AS-intercalated Co/Al-LDH; (f) DS-intercalated Ni/Al-LDH synthesized by the urea hydrolysis method aging for 24 h at 150 °C.

Table 5
Indexing of XRD patterns for Mg/Al-LDHs synthesized in 0.015 M SDS solution by the urea hydrolysis method aging for different time

Aging time (h)	d_{003} (nm)	d_{006} (nm)	d_{009} (nm)	d_{110} (nm)	Mg/Al molar ratio
1	3.32				0.02
2	2.77[a]	1.34[a]	0.889[a]	0.1515	0.86
6	2.77[a]/0.769[b]	1.33[a]/0.381[b]	0.860[a]	0.1519	1.71
12	2.73[a]/0.769[b]	1.31[a]/0.382[b]	0.858[a]	0.1524	2.07
24	2.77[a]/0.767[b]	1.31[a]/0.381[b]	0.868[a]	0.1525	2.09
120	0.748[b]	0.376[b]		0.1519	2.02

[a] (0 0 *l*) of DS anion-intercalated LDHs.
[b] (0 0 *l*) of CO_3^{2-} anion-intercalated LDHs.

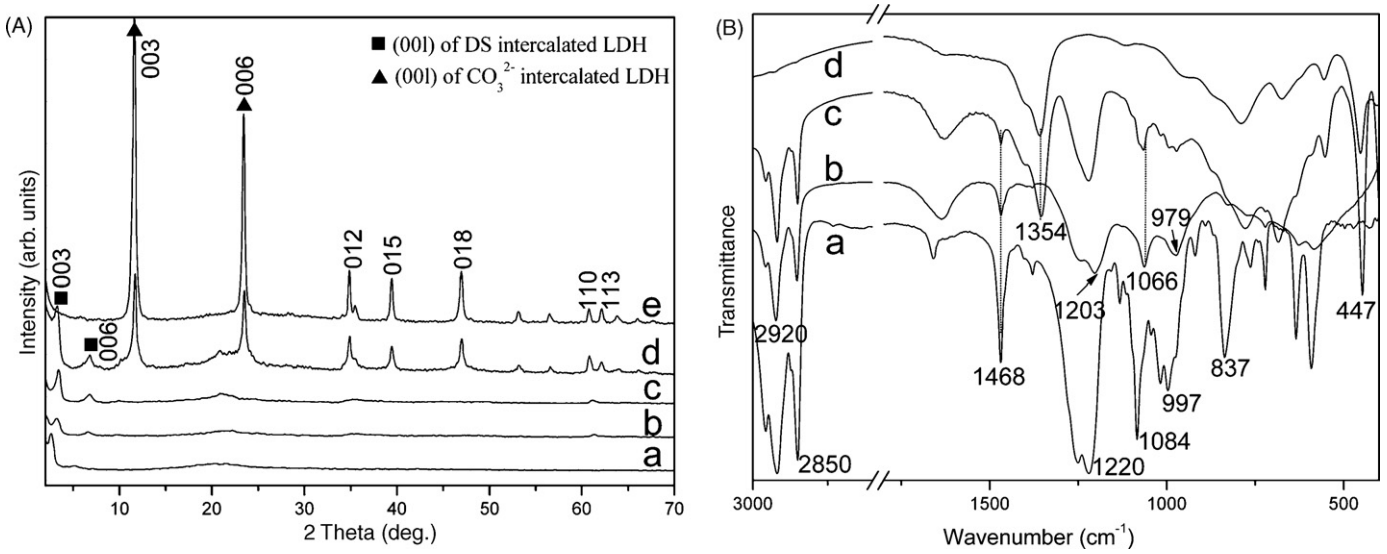

Fig. 6. (A) XRD patterns of Mg/Al-LDHs aging at 150 °C for (a) 1 h; (b) 2 h; (c) 3 h; (d) 24 h; (e) 120 h, respectively, in 0.02 M SDS solution by the urea hydrolysis method. (B) FT-IR spectra of pure SDS (a) and Mg/Al-LDHs aging at 150 °C for (b) 1 h; (c) 24 h; (d) 120 h.

and Ni/Al-LDHs, respectively. The co-existing CO_3^{2-}-LDH phase is also observed in each case for DS-intercalated LDHs. For AS-intercalated Mg/Al-LDH (Fig. 4a), the appearance of non-basal (0015), (0018) and (0021) reflections clearly exhibits the highly crystallized layered structure. It can be clearly observed that Co/Al-LDH and Ni/Al-LDH are less well ordered than Mg/Al-LDH. It can be well explained by the difference in cation radius and M–O bond length. The ion radius of Al^{3+}, Mg^{2+}, Co^{2+} and Ni^{2+} is 0.50, 0.65, 0.74 and 0.72 Å, respectively. The bond length of Al–O, Mg–O, Co–O and Ni–O is approximately 0.182, 0.197, 0.206, and 0.204 nm, respectively. The Co–O or Ni–O length deviates from Al–O more than Mg–O. More difference in the ion radius and M–O bond length, more difficult to form a well ordered structure.

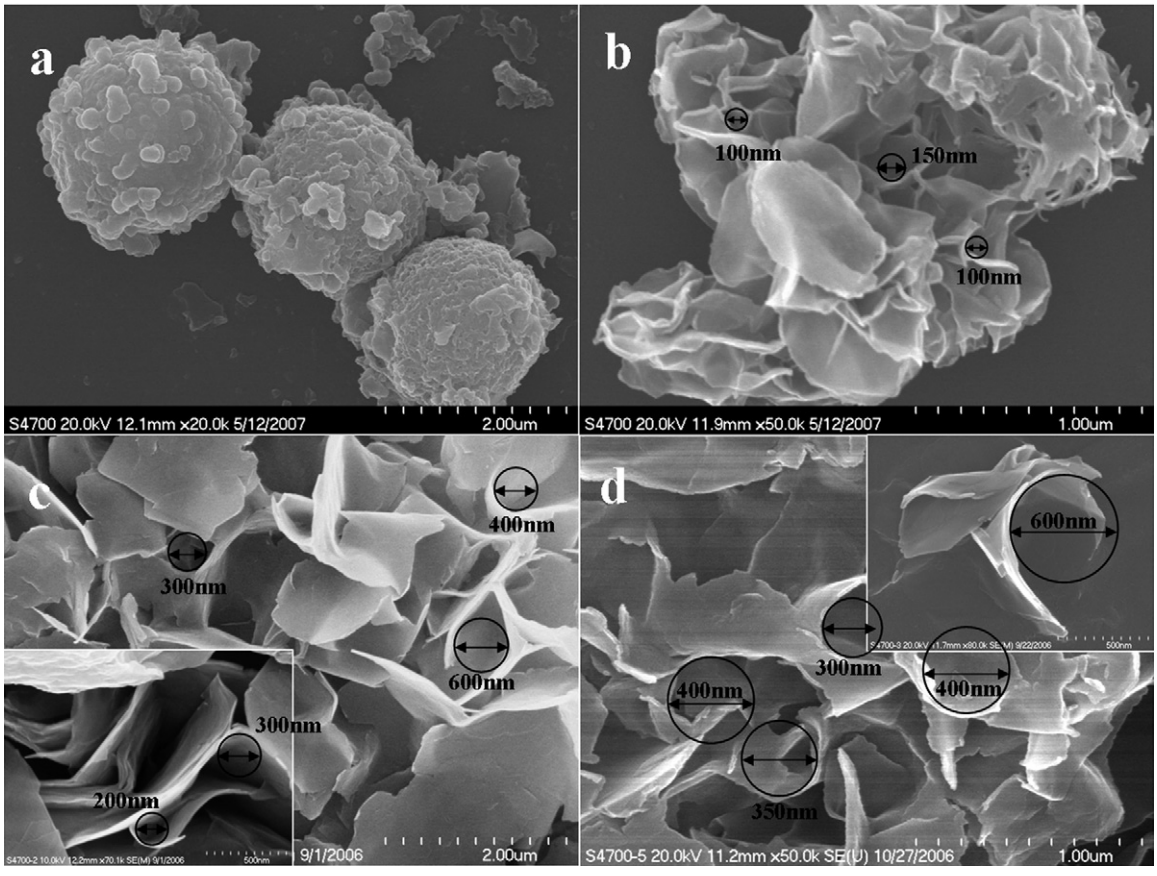

Fig. 7. SEM images of Mg/Al-LDHs aging at 150 °C for (a) 1 h; (b) 3 h; (c) 24 h; (d) 120 h, respectively, by the urea hydrolysis method.

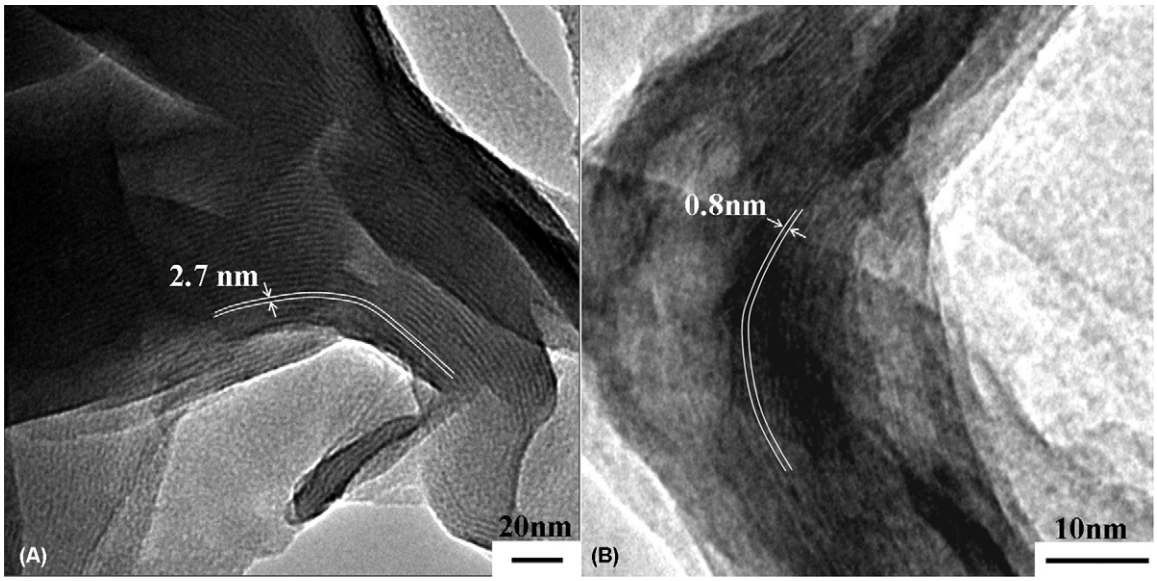

Fig. 8. TEM images of Mg/Al-LDHs aging at 150 °C for (a) 3 h; (b) 120 h in 0.02 M SDS solution by the urea hydrolysis method.

Table 2 gives the lattice parameters. Subtracting the thickness of LDH layer from the basal spacing, the interlayer spacing observed is all higher than the full length of the corresponding surfactant anion (2.08 nm for DS, 1.85 nm for AS [50] and 1.29 nm for AOT [51]). The observed basal spacing indicates a bilayer perpendicular arrangement of interlayer anions with the alkyl chains partially interdigitating for DS and AS, but a bilayer arrangement [52] with its two alkyl chains 55° leaning to LDHs' sheet for interlayer AOT anion. From the SEM images of the LDHs particles shown in Fig. 5, it can be seen that Mg/Al-LDHs particles with layer-bended or curved

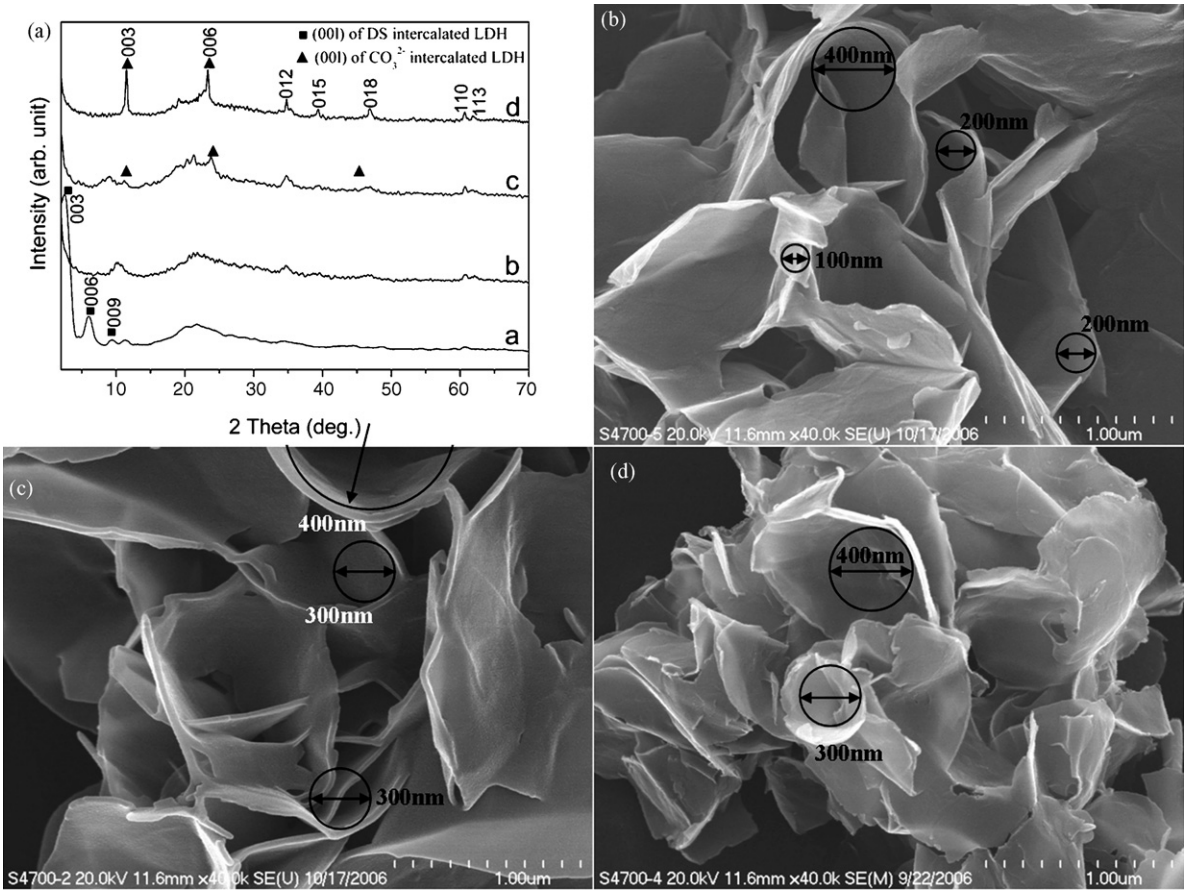

Fig. 9. XRD patterns and SEM images of the Mg/Al-LDHs synthesized in 0.002 M Mg^{2+} and 0.001 M Al^{3+} solution aging at 150 °C for (a) 24 h; (b) 48 h; (c) 72 h; (d) 120 h by the urea hydrolysis method.

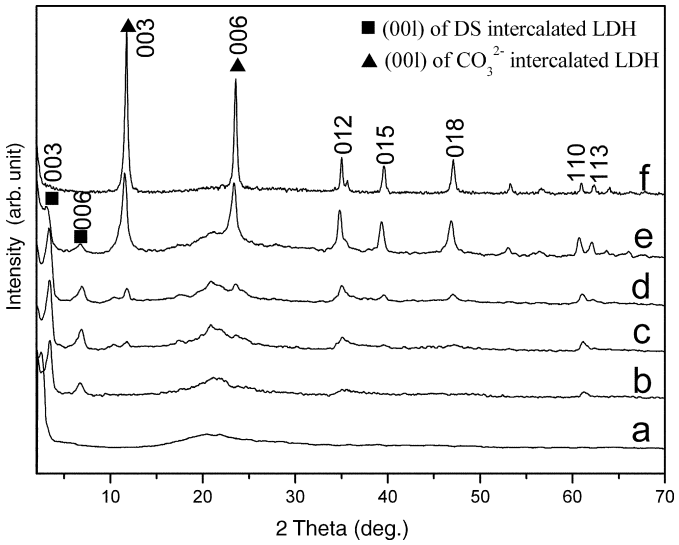

Fig. 10. XRD patterns of Mg/Al-LDHs aging at 150 °C for (a) 1 h; (b) 2 h; (c) 6 h; (d) 12 h; (e) 24 h; (f) 120 h in 0.015 M SDS solution by the urea hydrolysis method.

morphology (Fig. 5a–c) are produced in all DS, AS and AOT aqueous solutions. With similar molecular structure and chemical property, the DS, AS and AOT anions play similar roles at the interfaces in inducing the curved growth of LDHs' layers. The sheet deformation also readily occurs to Co/Al and Ni/Al-LDH (Fig. 5d–f), suggesting that the layer flexibility is of generalization for LDHs materials. But the deformation degree or curvature radius differs dependently on the surfactant anion and chemical composition of LDH sheets. The sheet of Co/Al-LDH (Fig. 5d) appears more difficult to bend than Mg/Al-LDH (Fig. 5b) and Ni/Al-LDH (Fig. 5f). On the same LDH sheet, Mg/Al for example (Fig. 5a–c), the deformation-inducing effects of different surfactants are different. The curvature radius of AS- or AOT-intercalated LDH (mostly 100 and 50 nm, respectively) is much smaller than that of DS-intercalated LDH (mostly 150 nm). So is the difference between AS- and DS-intercalated Co/Al-LDHs. This is proposed to result from the weaker interfacial interaction of DS than AS or AOT with positively charged sheets. The weak interfacial interaction works less on the inducing growth of LDHs layer, and also facilitates the ion exchange by CO_3^{2-}.

For DS-intercalated Mg/Al-, Co/Al-LDHs and Ni/Al-LDHs, (0 0 *l*) reflections of CO_3^{2-}-LDH are also observed (Fig. 4b, d and f and Table 2). The formation of CO_3^{2-}-LDH phase could arise from either the direct intercalation of CO_3^{2-} that commonly occurs in the urea hydrolysis method, or the secondary exchange of interlayer anions by CO_3^{2-}. It is to be further discussed in the following context.

3.2. Layer-bended Mg/Al-CO_3^{2-} LDH through exchange of interlayer anions

Mg/Al-LDHs were synthesized by the urea hydrolysis method for various aging time to investigate the formation process of bent layers. In urea hydrolysis method, it has been recognized that amorphous aluminum hydroxide is firstly formed and then convert into LDH crystals in further aging because of the lower precipitation pH of Al^{3+} than Mg^{2+} [14,17]. As observed in Fig. 6(A) and Table 3, DS-pillared amorphous Al hydroxide is formed firstly in 1 h aging, giving a basal spacing of 3.21 nm but no (1 1 0) reflection characteristic of LDH layers present. DS-intercalated LDHs structure appears in further aging, corresponding to the two-step process of LDHs formation by the urea hydrolysis method. With extended aging time, (0 0 *l*) reflections of CO_3^{2-}-LDHs appear, and at the same time (0 0 *l*) reflections of DS-LDHs weaken and disappear finally. Pure CO_3^{2-}-LDHs phase is produced in 120 h aging. The transformation of LDH structure observed in the aging period illustrates that the intercalation of CO_3^{2-} occurs only in an extended aging time, indicative of a possible formation of CO_3^{2-}-LDH through subsequent ion exchange. In the FT-IR spectra (Fig. 6 (B)), the encapsulation of $C_{12}H_{25}SO_4^-$ in LDH interlayer gallery causes a shift of the anti-symmetric and symmetric stretching vibrations of S=O from 1220 and 1084 cm^{-1} to 1203 and 1066 cm^{-1}, respectively. The weakening intensities of CH_2 stretching and C–H bending vibrations at 2920, 2850 and 1468 cm^{-1} reflect that the content of surfactant anion decreases with extended aging time. After 120 h aging, the anti-symmetric and symmetric stretching vibrations of S=O disappear. Simultaneously, the band at 1354 cm^{-1} related to the interlayer CO_3^{2-} anion is observed. The results show that dodecylsulfate anions in the gallery have been completely exchanged by CO_3^{2-}, consistent with XRD observation. Fig. 7 shows the morphology change of LDHs particles with extended aging time. Spherical aggregates of amorphous Al hydroxide are observed firstly. Layer-curved or bended LDH phase emerges later, and the bent layer morphology is kept even when all of interlayer DS anions have been completely exchanged by CO_3^{2-}. With extended aging time, the width of LDH sheet increases. But from Fig. 2d and Fig. 7b–d, it is obvious that the curvature radius increases from mostly 50–100 nm to mostly 200 nm with extended aging time, indicating the reduction of the deformation degree. It could be attributed to the higher rigidity of CO_3^{2-}-LDH slabs. HRTEM images (Fig. 8 and Fig. S2) prove that the bent sheets not only originate from primary crystals rather than particle aggregates, but also are continuous without breaks. After 3 h aging, sheet-curved LDHs show a basal spacing of 2.7 nm, consistent with XRD observation (Fig. 6(A)). After 120 h aging, sheet-curved LDHs display a basal spacing of about 0.8 nm. This observation suggests that the sheet-bended structure is stable during the great decrease in basal spacing.

Generally, decreasing the concentration of metal ions or extending aging time leads to larger LDH crystal size. [15,16] Therefore, the synthesis of Mg/Al-LDHs in 0.02 M SDS solution was performed in a decreased metal ion concentration (0.002 M Mg^{2+} and 0.001 M Al^{3+}) to discuss the change of crystal size and morphology. The XRD analysis (Fig. 9 and Table 4) shows that the exchange of interlayer DS anion by CO_3^{2-} has been retarded from 24 to 48 h by reducing the metal ion concentration. Fig. 9 also shows the SEM images of LDHs particles aged for different extents in low metal ion concentration. Comparing the particle size after 120 h aging under the two metal ion concentrations (Fig. 7d and Fig. 9d), little change in the crystal length and thickness have been observed, different from conventionally observed. It is the presence of surfactant anion that inhibits the growth of LDHs nuclei and crystals. The increase in particle width with aging time has been observed in Fig. 7. But with low metal ion concentration, extending aging time results in little change of the particle width, which is attributed to much more superfluous DS anion in the synthesis solution.

It has been found in Fig. 2 that sand-rose-like LDHs aggregates are formed when [SDS] ≤ 0.015 M (0.01 and 0.015 M herein). Although this kind of aggregate morphology has been observed in the previous studies [53,54], the aggregation mechanism is still undefined. The formation process of this special morphology is revealed in this work. As shown in Fig. 10 and Table 5, DS pillared Al hydroxide phase with a basal spacing of 3.32 nm is formed firstly in 1 h aging, similar to what is observed in Fig. 6A. Further aging results in the formation of LDHs' structure intercalated with DS anion. ICP analysis (Table 5) shows that with extending aging time, the Mg/Al molar ratio of LDHs layers increases from

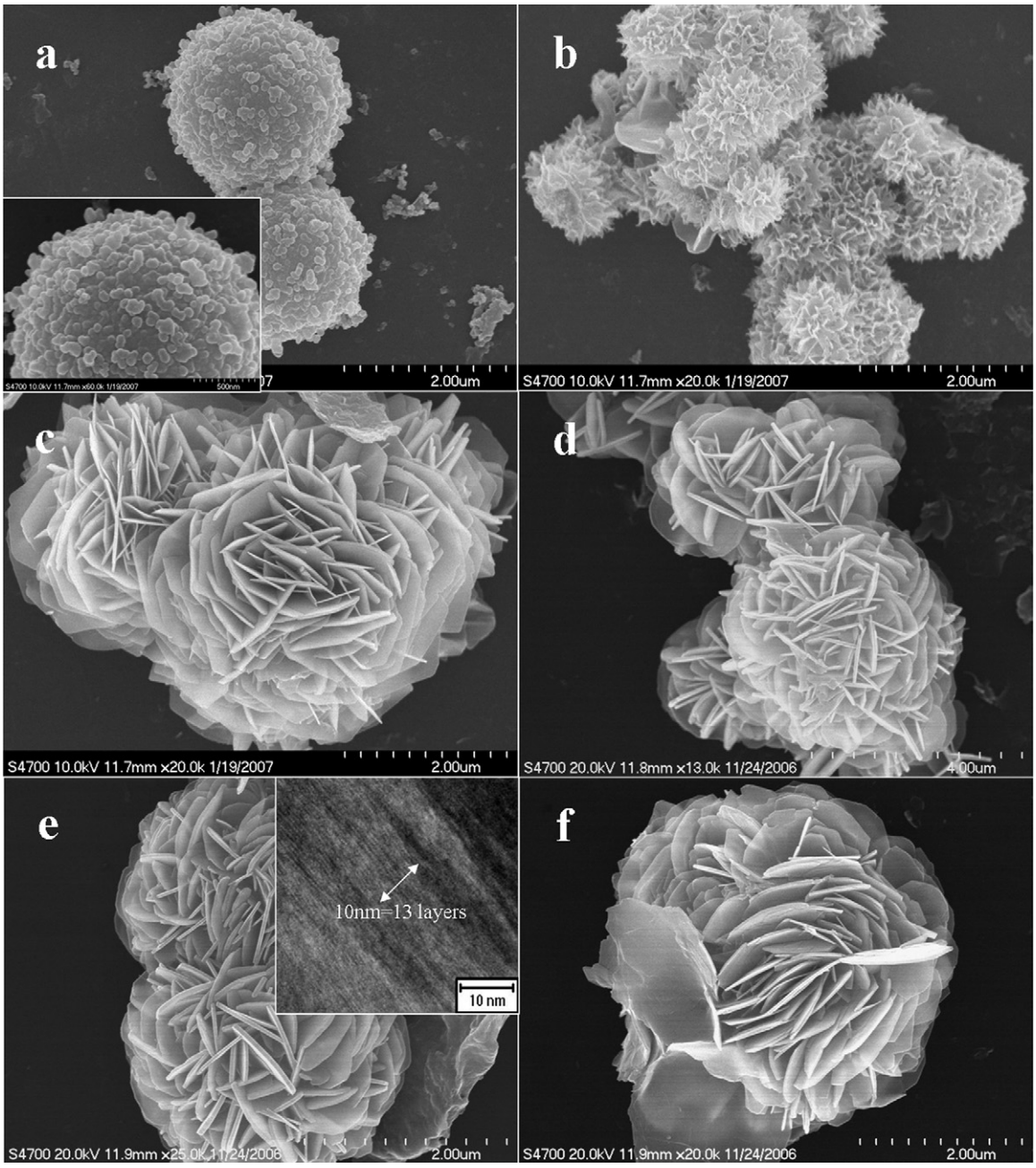

Fig. 11. SEM images of Mg/Al-LDHs aging at 150 °C for (a) 1 h; (b) 2 h; (c) 6 h; (d) 12 h; (e) 24 h; (f) 120 h in 0.015 M SDS solution by the urea hydrolysis method.

nearly zero to 2, corresponding to the two-step mechanism in the urea hydrolysis method. Similar to the structure change in 0.02 M SDS solution (Fig. 6A and Table 3), the (0 0 *l*) reflections of DS-intercalated LDHs weaken and finally disappear. The (0 0 *l*) reflections of CO_3^{2-}-intercalated LDHs accordingly appear with extending aging time. In 120 h aging, only CO_3^{2-}-intercalated LDHs is observed. The morphology change of LDHs with extended aging time, shown in Fig. 11, indicates that the spherical aggregates of small plate-like amorphous Al hydroxide are formed firstly. DS-intercalated LDHs with planar plate-like morphology are formed later and grow in the sphere. Sand-rose-like aggregate and sheet-planar particle morphology keep stable during the transformation of interlayer anion from DS to carbonate anion. But the LDH particles become thinner in stacking direction due to the great change of basal spacing.

Table 6
Indexing of XRD patterns for Mg/Al-LDHs synthesized in 0.02 M SDS solution by the co-precipitation method

Aging time (h)	d_{003} (nm)	d_{006} (nm)	d_{009} (nm)	d_{110} (nm)
24	2.68[a]	1.34[a]	0.891[a]	0.1518
72	2.62[a]/1.08[b]	1.31[a]/0.538[b]	0.890[a]/0.36[b]	0.1518
240	0.893[b]	0.444[b]		0.1518

[a] (0 0 *l*) of DS anion-intercalated LDH.
[b] (0 0 *l*) of SO_4^{2-} anion-intercalated LDH.

By the urea hydrolysis method, both of layer-curved and conventional plate-like LDHs particles are synthesized using surfactant anions as both intercalating candidate and growth-inducing template. Regardless of bent or planar LDH sheets, the particle morphology keeps stable in the transformation of

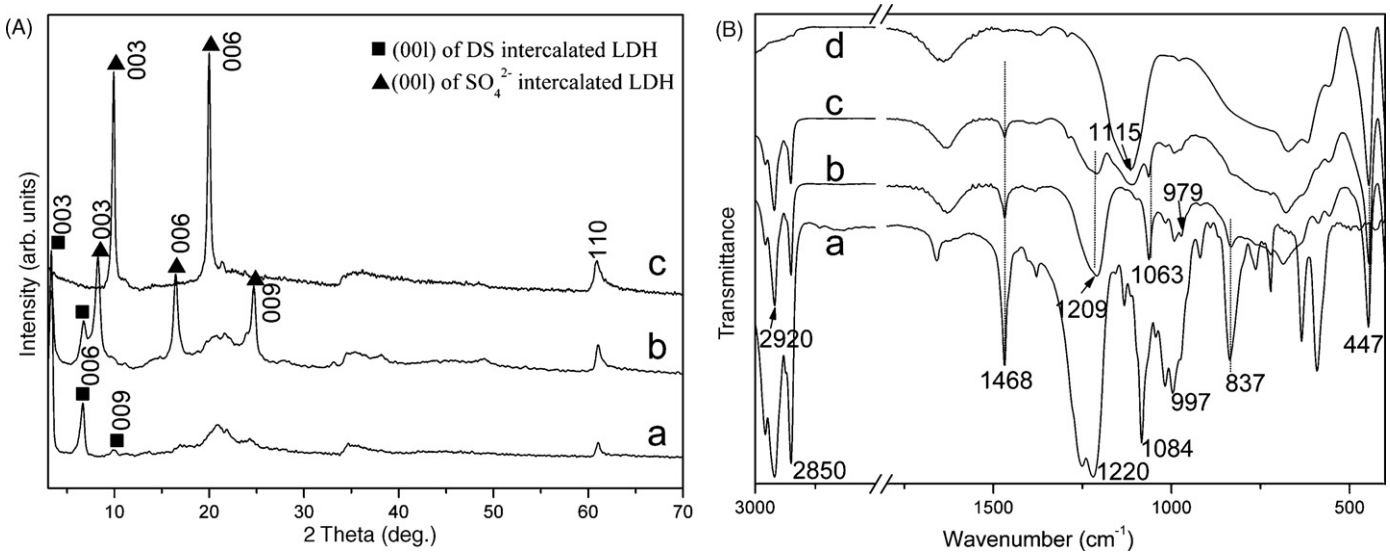

Fig. 12. (A) XRD patterns of Mg/Al-LDHs aging at 150 °C for (a) 24 h; (b) 72 h; (c) 240 h in 0.02 M SDS solution by the co-precipitation method. (B) FT-IR spectra of pure SDS (a) and Mg/Al-LDHs aging for (b) 24 h; (c) 72 h; (d) 240 h.

interlayer anion from long-chain surfactant anion to small inorganic CO_3^{2-} anion. Layer-bended Mg/Al-CO_3^{2-} LDH is produced by use of the flexibility of LDHs layers as well as the flexibility stability, which is difficult to achieve by a direct synthesis approach.

3.3. Layer-bended Mg/Al-SO_4^{2-} LDH through in situ decomposition of interlayer anions

The co-precipitation method has also been used to synthesize Mg/Al-LDHs in 0.02 M SDS concentration. Fig. 12 (A) shows the

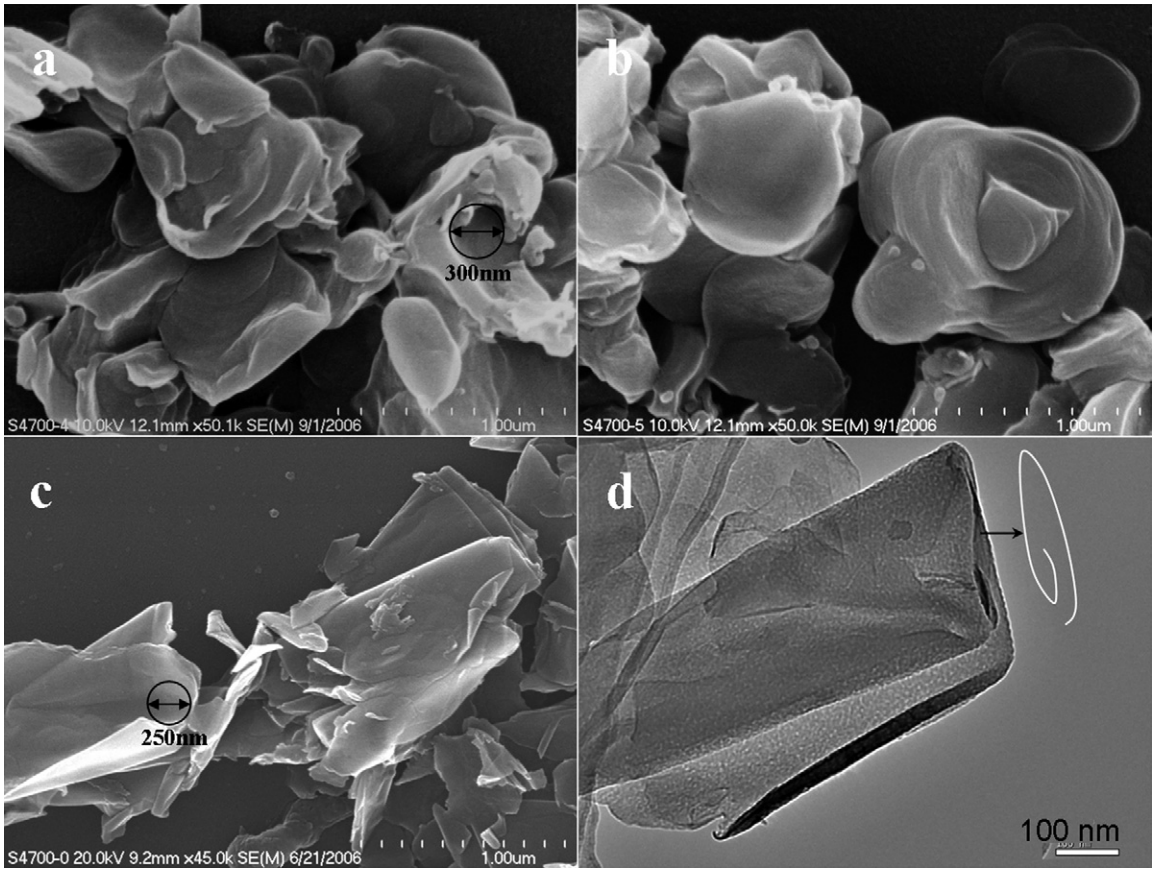

Fig. 13. SEM images of Mg/Al-LDHs aging at 150 °C for (a) 24 h; (b) 72 h; (c) 240 h in 0.02 M SDS solution by the co-precipitation method; (d) TEM image of (c).

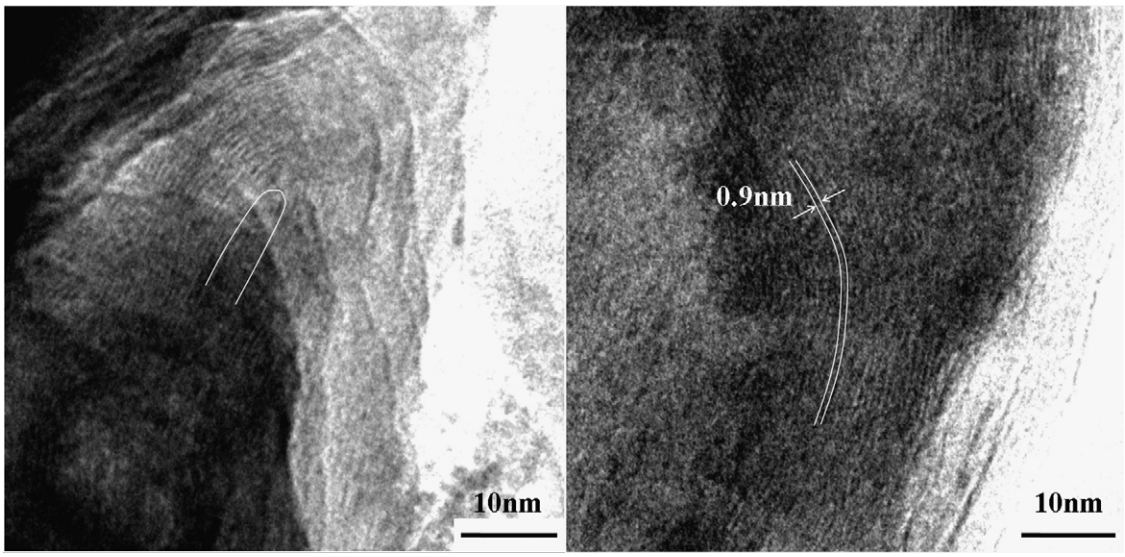

Fig. 14. TEM images of Mg/Al-LDHs aging at 150 °C for (a) 24 h; (b) 240 h in 0.02 M SDS solution by the co-precipitation method.

XRD patterns of LDHs synthesized at 150 °C for 24, 72 and 240 h, respectively. In 24 h aging, the XRD pattern displays (0 0 3), (0 0 6), (0 0 9) and (1 1 0) reflections characteristic of DS-intercalated LDHs. Extending the aging time, the (0 0 *l*) reflections typical of SO_4^{2-}-intercalated LDHs appear and shift to smaller basal spacing. The (0 0 *l*) reflections of DS-intercalated LDHs simultaneously weaken and finally disappear in 240 h aging. Table 6 gives the detailed lattice parameters of LDHs products. The two different d_{003} for SO_4^{2-}-LDHs (1.08 and 0.893 nm) can be explained by the change of water vapor pressure during the hydrothermal treatment, which has been discussed by Mostarih et al. [55]. The final SO_4^{2-} pillared LDH shows high crystallinity without other phase observed. It is a new route to synthesize SO_4^{2-}-LDH through *in situ* transformation of interlayer anions.

The FT-IR spectra (Fig. 12(B)) further testify the transformation process of interlayer anions. Similar to that observed in the urea

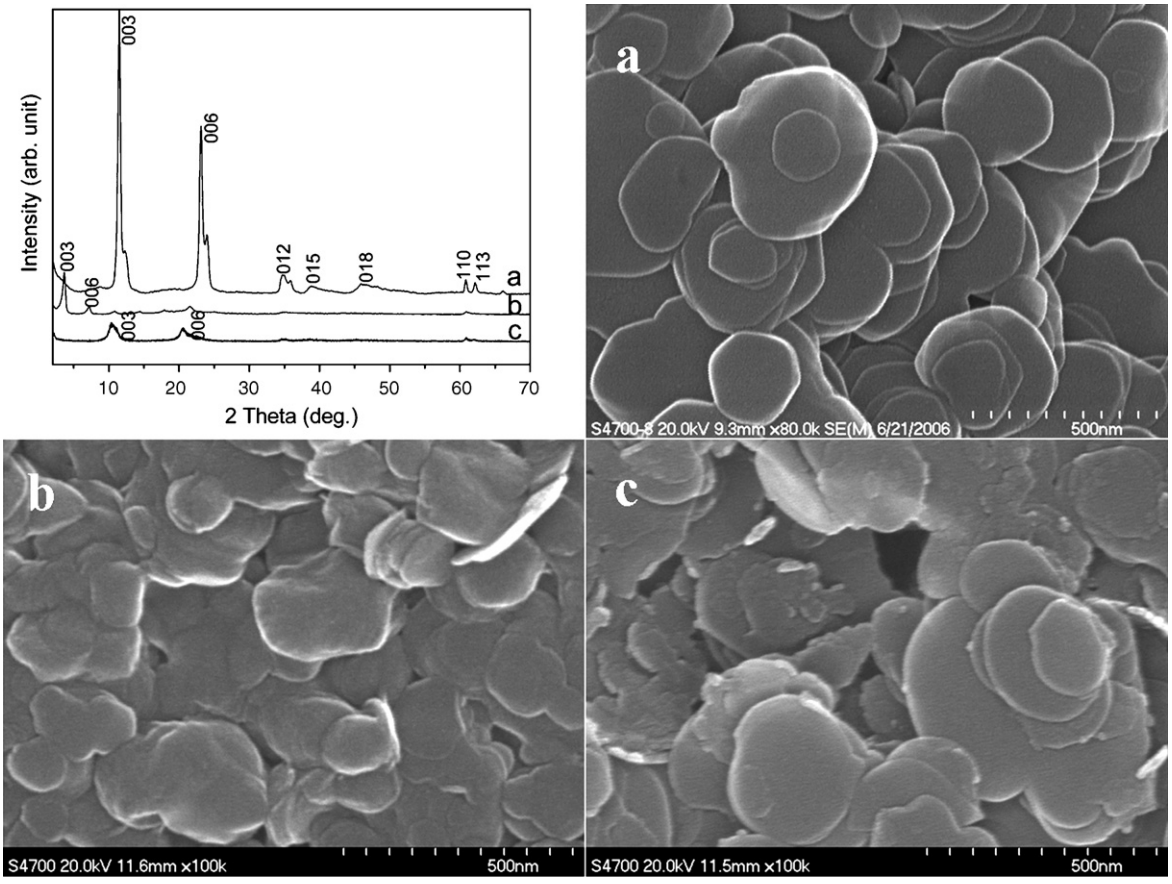

Fig. 15. XRD patterns and SEM images of (a) Mg/Al-CO_3^{2-} LDH; (b) Mg/Al-DS LDH prepared from ion-exchange of Mg/Al-SO_4^{2-} LDH by DS anion; (c) Mg/Al-SO_4^{2-} LDH.

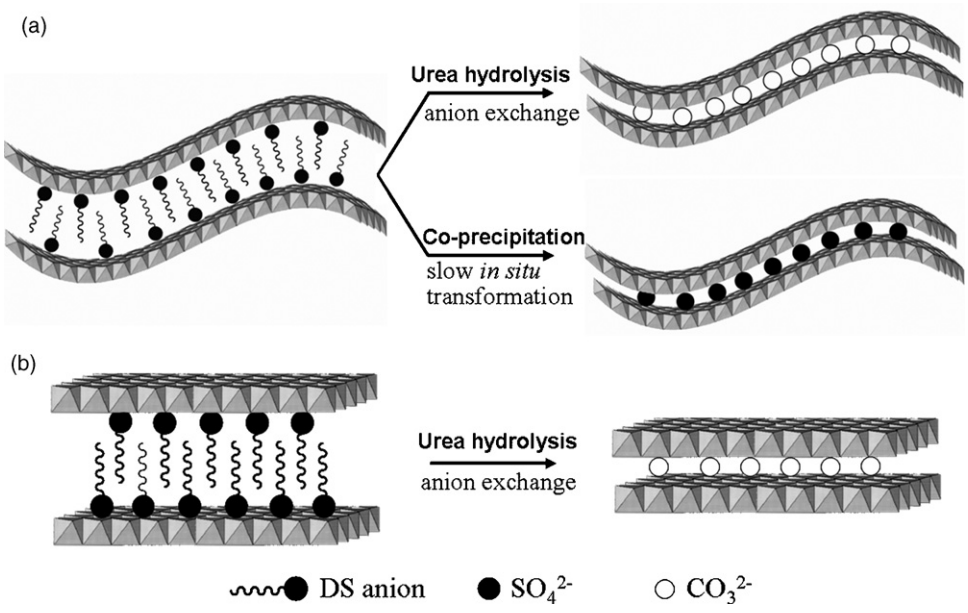

Fig. 16. Schematic illustration of the interlayer anion transformation of LDHs with (a) bent and (b) planar layers. Urea hydroxide method: DS anion would be directly exchanged by CO_3^{2-}; co-precipitation method: DS is decomposed to SO_4^{2-}, resulting in SO_4^{2-} pillared LDH. During the interlayer anion transformation, the morphology of LDHs is retained.

hydrolysis method, the CH_2 stretching and C–H bending vibrations (at 2920, 2850 and 1468 cm^{-1}) weaken with extending aging time, reflecting that the content of surfactant anion decreases. After 240 h aging, the anti-symmetric and symmetric stretching vibrations of S=O disappear. Simultaneously, the band at 1115 cm^{-1} related to inorganic SO_4^{2-} anion is observed. The results show that the alkyl group of dodecylsulfate anions in the interlayer gallery has been decomposed. As a result, SO_4^{2-} pillared LDH structure is formed finally, consistent with XRD observation.

Fig. 13 shows the SEM and TEM images of Mg/Al-LDHs particles synthesized by the co-precipitation method. The particles sizes are larger than 1 μm after 24 h or longer aging, and increase with extended aging time. The camber degree of the particles aged for 24 h is about 60–90° (Fig. 13a). Aging for 240 h, folded or even helical-like sheets can be observed clearly (Fig. 13c) for SO_4^{2-} pillared LDH. TEM image (Fig. 13d) clearly shows that the bended or curved shape originates from the single crystals rather than the particle aggregation. The slow *in situ* decomposition of dodecylsulfate group results in great reduction of stacking thickness and much more bending of LDHs' sheets. HRTEM images (Fig. 14 and Fig. S3) further prove that the bent sheets are continuous without breaks. The basal spacing is about 0.9 nm.

To prove that the layer bending is transferred from DS-LDH to the ion-exchanged samples, Mg/Al-CO_3^{2-} LDH and Mg/Al-SO_4^{2-} LDH as precursors have been synthesized and then aged in 0.02 M SDS solution. As shown in Fig. 15, after 24 h aging in SDS solution, well-crystallized Mg/Al-CO_3^{2-} LDH is retained. But Mg/Al-SO_4^{2-} has been exchanged to Mg/Al-DS LDHs. SEM images show that all the samples display typical sheet-planar morphology. No bent particles are observed. This phenomenon suggests that the layer bending requires the simultaneous occurrence of intercalation and interfacial template of DS anions. No bending could be induced by DS anions in the post-synthesis ion exchange even though the interlayer sulfate has been transformed to DS anion.

Crepaldi et al. [43] has reported that the interlayer DS anion begins to degrade at 150 °C. The decomposition starts by the breaking of the head-tail bond and sulfate is formed firstly. But SO_4^{2-}-intercalated LDH structure was not observed in their work. In this work however, two instances are turned out. In the co-precipitation method, SO_4^{2-}-intercalated LDH phase is clearly observed because no competent anions for secondary ion exchange exist in the system. But in the urea hydrolysis method, no SO_4^{2-}-intercalated LDH is observed, which is supposed to be a consequence of plenty of CO_3^{2-} in the synthesis mixture. The formation of inorganic-pillared LDHs and morphology stability of flexible LDHs' layers are schematically illustrated in Fig. 16. Although only DS-intercalated and CO_3^{2-}-intercalated LDHs structures are observed in the urea hydrolysis method as discussed in Section 3.2, one might wonder that SO_4^{2-}-LDH probably ever emerges as a transitory phase and then instantaneously transforms to CO_3^{2-}-LDH. But it can be seen from Fig. 17, which illustrates the summary of the morphology and crystal phase of LDHs obtained

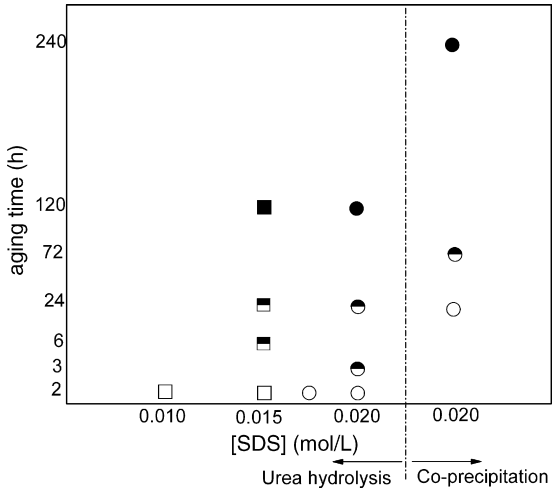

Fig. 17. Sketch illustration of crystal phase and morphology of LDHs obtained in this work. (□) and (○) represent the organic-intercalated LDHs with plate-like and bent sheets, respectively; (■) and (●) represent the inorganic-intercalated LDHs with plate-like and bent sheets, respectively; and the white-black symbols represent the co-existence of organic and inorganic-intercalated LDHs.

under various conditions, no decomposition of DS has occurred at 24 h when CO_3^{2-}-LDH emerges. The SO_4^{2-}-LDH phase has not been formed until 72 h aging. The process of *in situ* decomposition is slower than CO_3^{2-} anion-exchange, which explains for more bent layers by the co-precipitation method.

4. Conclusion

In summary, sheet-curved or bended LDHs have been synthesized using anionic surfactants as both interlayer anions and growth-inducing template for LDHs nuclei, experimentally confirming the flexibility of LDHs' host layers. Through *in situ* transformation and ion exchange of interlayer anions, SO_4^{2-}- or CO_3^{2-}-intercalated LDHs retaining the layer-bended morphology of Mg/Al-DS LDHs precursor are produced.

Acknowledgments

The authors are grateful to the financial support from NSFC, Program for Changjiang Scholars and Innovative Research Team in University (IRT0406), Program for New Century Excellent Talents in University (NCET-04-0119) and "111" Project (B07004).

Appendix A. Supplementary data

Supplementary data associated with this article can be found, in the online version, at doi:10.1016/j.cej.2008.06.031.

References

[1] C.C. Tsai, T.Y. Juang, S.A. Dai, T.M. Wu, W.C. Su, Y.L. Liu, R.J. Jeng, Synthesis and montmorillonite-intercalated behavior of dendritic surfactants, J. Mater. Chem. 16 (2006) 2056–2063.
[2] J.Y. Huang, H. Yasuda, H. Mori, Highly curved carbon nanostructures produced by ball-milling, Chem. Phys. Lett. 303 (1999) 130–132.
[3] Y. Tan, S. Srinivasan, K.S. Choi, Electrochemical deposition of mesoporous nickel hydroxide films from dilute surfactant solutions, J. Am. Chem. Soc. 127 (2005) 3596–3604.
[4] J. He, T. Kunitale, Are ceramic nanofilms a soft matter, Soft Mater. 2 (2006) 119–125.
[5] N. Daumas, A. Hérold, Relations between the elementary stage and the reaction mechanisms in graphite insertion compounds, C.R. Seances Acad. Sci. Ser. C 268 (1969) 373–375.
[6] M.E. Misenheimer, H. Zabel, Stage transformation and staging disorder in graphite intercalation compounds, Phys. Rev. Lett. 54 (1985) 2521–2524.
[7] J. Pisson, C. Taviot-Guého, Y. Israëli, F. Leroux, P. Munsch, J.P. Itié, V. Briois, N. Morel-Desrosiers, J.P. Besse, Staging of organic and inorganic anions in layered double hydroxides, J. Phys. Chem. B 107 (2003) 9243–9248.
[8] V. Rives, Layered Double Hydroxides: Present and Future, Nova Science Publishers, New York, 2001.
[9] D.G. Evans, R.C.T. Slade, Structural aspects of layered double hydroxides, Struct. Bond. 119 (2006) 1–87.
[10] F. Cavani, F. Trifiro, A. Vaccari, Hydrotalcite-type anionic clays: preparation, properties and applications, Catal. Today 11 (1991) 173–301.
[11] P.S. Braterman, Z.P. Xu, F. Yarberry, Layered double hydroxides (LDHs), in: S.M. Auerbach, K.A. Carrado, P.K. Dutta (Eds.), Handbook of Layered Materials, Marcel Dekker, Inc., New York, Basel, 2004, pp. 373–474.
[12] D.G. Evans, X. Duan, Preparation of layered double hydroxides and their applications as additives in polymers, as precursors to magnetic materials and in biology and medicine, Chem. Commun. 6 (2006) 485–496.
[13] G.R. Williams, D. O'Hare, Towards understanding, control and application of layered double hydroxide chemistry, J. Mater. Chem. 16 (2006) 3065–3074.
[14] U. Costantino, F. Marmottini, M. Nocchetti, R. Vivani, New synthetic routes to hydrotalcite-like compounds-characterisation and properties of the obtained materials, Eur. J. Inorg. Chem. (1998) 1439–1446.
[15] J.M. Oh, S.H. Hwang, J.H. Choy, The effect of synthetic conditions on tailoring the size of hydrotalcite particles, Solid State Ionic 151 (2002) 285–291.
[16] M. Ogawa, H. Kaiho, Homogeneous precipitation of uniform hydrotalcite particles, Langmuir 18 (2002) 4240–4242.
[17] M. Adachi-Pagano, C. Forano, J.P. Besse, Synthesis of Al-rich hydrotalcite-like compounds by using the urea hydrolysis reaction-control of size and morphology, J. Mater. Chem. 13 (2003) 1988–1993.
[18] Y. Zhao, F. Li, R. Zhang, D.G. Evans, X. Duan, Preparation of layered double-hydroxide nanomaterials with a uniform crystallite size using a new method involving separate nucleation and aging steps, Chem. Mater. 14 (2002) 4286–4291.
[19] S. Miyata, Anion-exchange properties of hydrotalcite-like compounds, Clay. Clay Miner. 31 (1983) 305–311.
[20] J. He, M. Wei, B. Li, Y. Kang, D.G. Evans, X. Duan, Preparation of layered double hydroxides, Struct. Bond. 119 (2006) 89–119.
[21] A.M. Fogg, J.S. Dunn, D. O'Hare, Formation of second-stage intermediates in anion-exchange intercalation reactions of the layered double hydroxide $[LiAl_2(OH)_6]Cl{\cdot}H_2O$ as observed by time-resolved, in situ X-ray diffraction, Chem. Mater. 10 (1998) 356–360.
[22] N. Iyi, K. Kurashima, T. Fujita, Orientation of an organic anion and second-staging structure in layered double-hydroxide intercalates, Chem. Mater. 14 (2002) 583–589.
[23] G.R. Williams, A.M. Fogg, J. Sloan, C. Taviot-Guého, D. O'Hare, Staging during anion-exchange intercalation into $[LiAl_2(OH)_6]Cl{\cdot}yH_2O$: structural and mechanistic insights, Dalton Trans. (2007) 3499–3506.
[24] S.A. Solin, D. Hines, S.K. Yun, T.J. Pinnavaia, M.F. Thorpe, Layer rigidity in 2D disordered Ni–Al layer double hydroxides, J. Non-Cryst. Solids 182 (1995) 212–220.
[25] D.R. Hines, S.A. Solin, U. Costantino, M. Nocchetti, Layer double hydroxides containing a fixed host-layer, Mol. Cryst. Liq. Cryst. 341 (2000) 377–382.
[26] W. Rüdorff, Reactions of electropositive metals with graphite and with metal dichalcogenides, Angew. Chem. Int. Edit. 5 (1966) 904.
[27] M.A. Thyveetil, P.V. Coveney, J.L. Suter, H.C. Greenwell, Emergence of undulations and determination of materials properties in large-scale molecular dynamics simulation of layered double hydroxides, Chem. Mater. 19 (2007) 5510–5523.
[28] F. Leroux, J.P. Besse, Polymer interleaved layered double hydroxide: a new emerging class of nanocomposites, Chem. Mater. 13 (2001) 3507–3515.
[29] S. Vial, V. Prevot, F. Lerous, C. Forano, Immobilization of urease in ZnAl layered double hydroxides by soft chemistry routes, Micropor. Mesopor. Mater. 107 (2008) 190–201.
[30] A.I. Khan, D. O'Hare, Intercalation chemistry of layered double hydroxides: recent developments and applications, J Mater. Chem. 12 (2002) 3191–3207.
[31] M. Darder, M. López-Blance, P. Aranda, F. Leroux, E. Ruiz-Hitzky, Bionanocomposites based on layered double hydroxides, Chem. Mater. 17 (2005) 1969–1977.
[32] F. Li, X. Duan, Applications of layered double hydroxides, Struct. Bond. 119 (2005) 193–223.
[33] Z. An, W.H. Zhang, H.M. Shi, J. He, An effective heterogeneous L-proline catalyst for the asymmetric aldol reaction using anionic clays as intercalated support, J. Catal. 241 (2006) 319–327.
[34] J. Comas, M.L. Dieuzeide, G. Baronetti, M. Laborde, N. Amadeo, Methane steam reforming and ethanol steam reforming using a Ni(II)–Al(III) catalyst prepared from lamellar double hydroxides, Chem. Eng. J. 118 (2006) 11–15.
[35] F. Yagiz, D. Kazan, A.N. Akin, Biodiesel production from waste oils by using lipase immobilized on hydrotalcite and zeolites, Chem. Eng. J. 134 (2007) 262–267.
[36] L. Desigaux, M.B. Belkacem, P. Richard, J. Cellier, P. Leone, L. Cario, F. Leroux, C. Taviot-Gueho, B. Pitard, Self-assembly and characterization of layered double hydroxide/DNA hybrids, Nano Lett. 6 (2006) 199–204.
[37] Y. You, H. Zhao, G.F. Vance, Hybrid organic–inorganic derivatives of layered double hydroxides and dodecylbenzenesulfonate: preparation and adsorption characteristics, J. Mater. Chem. 12 (2002) 907–912.
[38] K. Melánová, L. Beneš, V. Zima, J. Svoboda, Intercalation of dyes containing SO_3H groups into Zn–Al layered double hydroxide, J. Incl. Phenom. Macro. Chem. 51 (2005) 97–101.
[39] H.J. Butt, K. Graf, M. Kappl, Physics and chemistry of interfaces, Wiley-VCH Verlag & Co. KGaA, Weinheim, 2003, p. 250.
[40] J.N. Israelachvili, D.J. Mitchell, B.W. Ninham, Theory of self-assembly of hydrocarbon amphiphiles into micelles and bilayers, J. Chem. Soc., Faraday Trans. 72 (1976) 1525–1568.
[41] B. Li, J. He, Multiple effects of dodecanesulfonate in the crystal growth control and morphosynthesis of layered double hydroxides, J. Phys. Chem. C 112 (2008) 10909–10917.
[42] E. Han, D. Shan, H. Xue, S. Cosnier, Hybrid material based on chitosan and layered double hydroxides: characterization and application to the design of amperometric phenol biosensor, Bimacomolecules 8 (2007) 971–975.
[43] E.L. Crepaldi, P.C. Pavan, J. Tronto, J.B. Valim, Chemical, structural, and thermal properties of Zn(II)–Cr(III) layered double hydroxides intercalated with sulfated and sulfonated surfactants, J. Colloid Interf. Sci. 248 (2002) 429–442.
[44] M. Meyn, K. Beneke, G. Lagaly, Anion-exchange reactions of layered double hydroxides, Inorg. Chem. 29 (1990) 5201–5207.
[45] A. Clearfield, M. Kieke, J. Kwan, J.L. Colon, R.C. Wang, Intercalation of dodecyl sulfate into layered double hydroxides, J. Inclus. Phenom. Mol. Recogn. Chem. 11 (1991) 361–378.
[46] H. Zhao, K.L. Nagy, Dodecyl sulfate–hydrotalcite nanocomposites for trapping chlorinated organic pollutants in water, J. Colloid Interf. Sci. 274 (2004) 613–624.
[47] F. Leroux, P. Aranda, J.-P. Besse, E. Ruiz-Hitzky, Intercalation of poly(ethylene oxide) derivatives into layered double hydroxides, Eur. J. Inorg. Chem. (2003) 1242–1251.

[48] M. Zammarano, S. Bellayer, J.W. Gilman, M. Franceschi, F.L. Beyer, R.H. Harris, S. Meriani, Delamination of organo-modified layered double hydroxides in polyamide 6 by melt processing, Polymer 47 (2006) 652–662.
[49] C. Jaubertie, M.J. Holgado, M.S. San Román, V. Rives, Structural characterization and delamination of lactate-intercalated Zn Al-layered double hydroxides, Chem. Mater. 18 (2006) 3114–3121.
[50] M.A. Drezdzon, Synthesis of isopolymetalate-pillared hydrotalcite via organic-anion-pillared precursors, Inorg. Chem. 27 (1988) 4628–4632.
[51] B.A. Simmons, C.E. Taylor, F.A. Landis, V.T. John, G.L. McPherson, D.K. Schwartz, R. Moore, Microstructure determination of AOT + phenol organogels utilizing small-angle X-ray scattering and atomic force microscopy, J. Am. Chem. Soc. 123 (2001) 2414–2421.
[52] M.Z.B. Hussein, T.K. Hwa, Synthesis and properties of layered organic-inorganic hybrid material: Zn–Al layered double hydroxide-dioctyl sulfosuccinate nanocomposite, J. Nanopart. Res. 2 (2000) 293–298.
[53] F. Leroux, J. Gachon, J.P. Besse, Biopolymer immobilization during the crystalline growth of layered double hydroxide, J. Solid State Chem. 177 (2004) 245–250.
[54] Z.P. Xu, G.Q. Lu, Hydrothermal synthesis of layered double hydroxides (LDHs) from mixed MgO and Al_2O_3: LDH formation mechanism, Chem. Mater. 17 (2005) 1055–1062.
[55] R. Mostarih, A. de Roy, Thermal behavior of a zinc–chromium–sulfate lamellar double hydroxide revisited as a function of vacuum and moisture parameters, J. Phys. Chem. Solid 67 (2006) 1058–1062.